

# Petrophysical Properties Evaluation of Tight Gas Sand Reservoirs Using NMR and Conventional Openhole Logs

G.M. Hamada\*

King Fahd University of Petroleum & Minerals, Saudi Arabia

**Abstract:** Tight reservoir means reservoir of low porosity and low permeability. Many tight formations are extremely complex, produced from multiple layers with different permeability that is often enhanced by natural fracturing. The complicity of these reservoirs is attributed to a) Low porosity and low permeability reservoir, b) The presence of clay minerals like illite, kaolin and micas in pores, c) The heterogeneity of the reservoir in vertical and lateral directions. Evaluation of tight gas sand reservoirs represents difficult problems. Determination of petrophysical properties using only conventional logs is very complicated. Use of NMR in individual bases or in combination with conventional openhole logs and SCAL data leads to better determination of petrophysical properties of heterogeneous tight gas sand reservoirs.

This paper focuses on determination of three petrophysical parameters of tight gas sand reservoirs: 1) Determination of detailed NMR porosity in combination with density porosity,  $\phi_{DMR}$ , 2) NMR permeability,  $K_{BGMR}$ , which is based on the dynamic concept of gas movement and bulk gas volume in the invaded zone and 3) Capillary pressure derived from relaxation time  $T_2$  distribution and then it could be used for the saturation formation measurements especially in the transition zone.

**Keywords:** Tight gas sand reservoirs, conventional logs, nuclear magnetic resonance log, porosity, permeability and capillary pressure.

## INTRODUCTION

The field of interest is gas condensate field, produced from the Lower-Mesozoic reservoir. The reservoir is classified as a tight heterogeneous gas shaly sands reservoir. It suffers from lateral and vertical heterogeneity due to diagenesis effect (Kaolinite & Illite) and variation in grain size distribution. The petrophysical analysis indicates narrow 8-12% porosity range while wide permeability ranges from 0.01 to 100 mD. Fig. (1) shows core porosity-permeability crossplot over whole reservoir section including all facies in different wells. The core data shows cloud of points with undefined trend, so, it is subdivided into six subunits. The uncertainty associated with identification of the proper porosity and permeability model for each unit is high, which could result in high permeability estimation far below the actual well performance. Therefore, integration on non-standard tools like NMR with conventional tools and SCAL in the petrophysical evaluation is essential to reduce the uncertainty beyond the limitations of each tool in individual bases, especially in gas reservoirs. The aim is to establish facies independent porosity and permeability models and avoid using lithology independent  $T_2$  cut-off. The advantage of NMR tool is sensitive only to hydrogen and fluid protons and no borehole correction is needed whenever the radius of investigation is beyond calliper measurements [1-3].

This work presents: 1) The application of Density Magnetic Resonance Porosity ( $\phi_{DMR}$ ) technique for porosity

calculation, 2) Bulk gas Magnetic Resonance Permeability ( $K_{BGMR}$ ), new technique for permeability calculation beyond the limits of OBM filtrate. 3) Quantify the effect of OBM filtrate on NMR data and then calibration for approximated capillary pressure from NMR. Although the big challenges associated with applications of NMR techniques, like reservoir heterogeneity, gas bearing sand and oil base mud (OBM) environment, the result are very encouraging and significantly reduced the petrophysical parameters uncertainties.

## DENSITY-MAGNETIC RESONANCE POROSITY ( $\phi_{DMR}$ )

Traditional determination of formation relies on porosity logs, mainly density and neutron. Porosity logs measurements require environmental corrections and are influenced by lithology and formation fluids. The porosity derived, is the total porosity, which consists of producible fluids, capillary bound water, and clay-bound water. However, NMR provides lithology independent porosity and includes only producible fluids and capillary bound water. In heterogeneous reservoirs having mixed or unknown lithology, NMR is highly recommended for an accurate porosity determination [4, 5].

Freedman *et al.* [6] proposed a combination of density porosity and NMR porosity ( $\phi_{DMR}$ ) to determine gas corrected porosity formation and flushed zone water saturation ( $S_{xo}$ ). Density/NMR crossplot is superior to density/neutron crossplot for detecting and evaluating gas shaly sands. This superiority is due to the effect of thermal neutron absorbers in shaly sands on neutron porosities, which cause neutron porosity readings too high. As a result neutron/density logs

\*Address correspondence to this author at the King Fahd University of Petroleum & Minerals, Saudi Arabia; E-mail: ghamada@kfupm.edu.sa

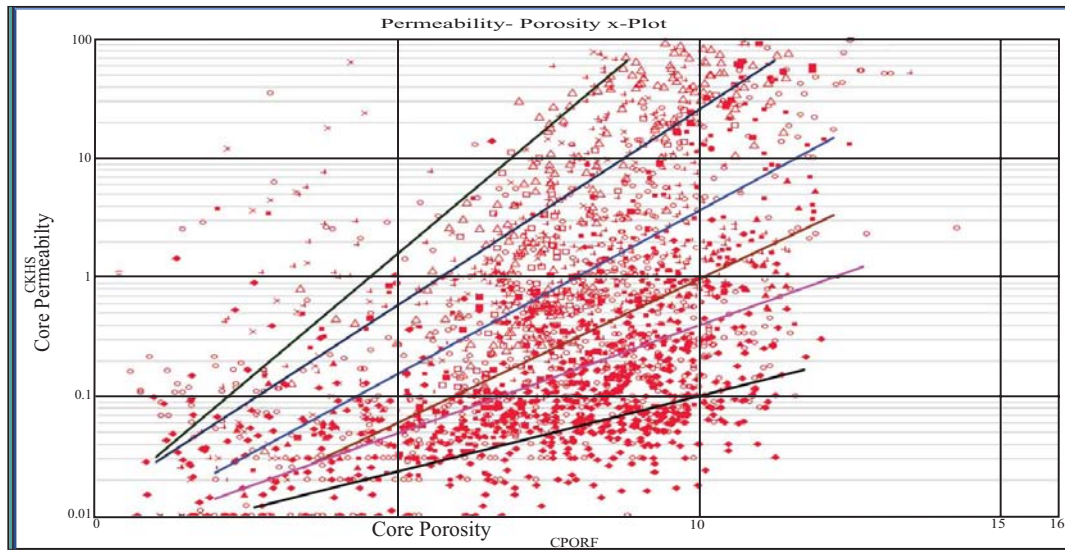


Fig. (1). Porosity-permeability plot in heterogeneous gas sand.

can miss gas zones in shaly sands [7]. On the other hand, NMR porosities are not affected by shale or rock mineralogy, and therefore density/ NMR (DMR) technique is more reliable to indicate and evaluate gas shaly sands.

**( $\phi_{DMR}$ ) Derivation**

Following is the derivation of density/ NMR porosity,  $\phi_{DMR}$ . It is assumed that both density and NMR tools read within the same gas flushed zone.

**NMR Porosity Response:** NMR porosity response in flushed gas zone is defined as:

$$\phi_{NMR} = \phi S_{gxo} HI_g P_g + \phi HI_L (1 - S_{gxo})$$

Assume hydrogen index for liquid ( $HI_L$ ) = 1

$$\phi_{NMR} = \phi * [1 - S_{gxo} (1 - HI_g P_g)]$$

$$\frac{\phi_{NMR}}{\phi} = 1 - S_{gxo} (1 - HI_g P_g) \tag{1}$$

Where;

- $\phi_{NMR}$  : Porosity of NMR tool
- $\phi$  : Gas corrected porosity
- $HI_g$ : gas hydrogen index
- $HI_L$  : fluid hydrogen index (water + mud filtrate)
- $S_{gxo}$  : gas saturation in the flushed zone
- $P_g = 1 - \exp(-W/T_{1,g})$ : gas polarization factor
- $W$  : wait time
- $T_{1,g}$  = gas longitudinal relaxation time.

**Density Porosity Response**

Density porosity response in gas flushed zone is defined as :

$$\rho_b = \rho_m (1 - \phi) + \rho_L \phi (1 - S_{gxo}) + \rho_g \phi S_{gxo}$$

$$\phi_D = \frac{\rho_m - \rho_b}{\rho_m - \rho_L} = \frac{\rho_m - [\rho_m (1 - \phi) + \rho_L \phi (1 - S_{gxo}) + \rho_g \phi S_{gxo}]}{\rho_m - \rho_L}$$

$$\phi_D = \phi [1 + S_{gxo} \left( \frac{\rho_L - \rho_g}{\rho_m - \rho_L} \right)] \tag{2}$$

Where;

- $\rho_b$  : Bulk Density
- $\rho_L$  : liquid Density (water + filtrate)
- $\phi_D$  : Apparent porosity from density
- $\rho_g$  : Gas Density

**Solution For Gas Corrected Porosity  $\phi$**

Assume constants  $\beta, \alpha$  where,

$$\beta = \frac{\rho_L - \rho_g}{\rho_m - \rho_L} \text{ and } \alpha = (1 - HI_g P_g)$$

Substitute in Eq. (1) & (2)

$$\frac{\phi_{NMR}}{\phi} = 1 - \alpha S_{gxo} \tag{3}$$

$$\frac{\phi_D}{\phi} = 1 + \beta S_{gxo} \tag{4}$$

Solution of Eq. 3 & 4 for True formation porosity ( $\phi$ )

$$\phi = \left( \frac{\alpha}{\beta + \alpha} * \phi_D + \frac{\beta}{\beta + \alpha} * \phi_{NMR} \right)$$

$$\phi = A * \phi_D + B * \phi_{NMR}$$

$$\phi_{DMR} = A * \phi_D + B * \phi_{NMR} \tag{5}$$

A& B are constant where

$$A + B = \frac{\alpha}{\beta + \alpha} + \frac{\beta}{\beta + \alpha} = \frac{\beta + \alpha}{\beta + \alpha} = 1$$

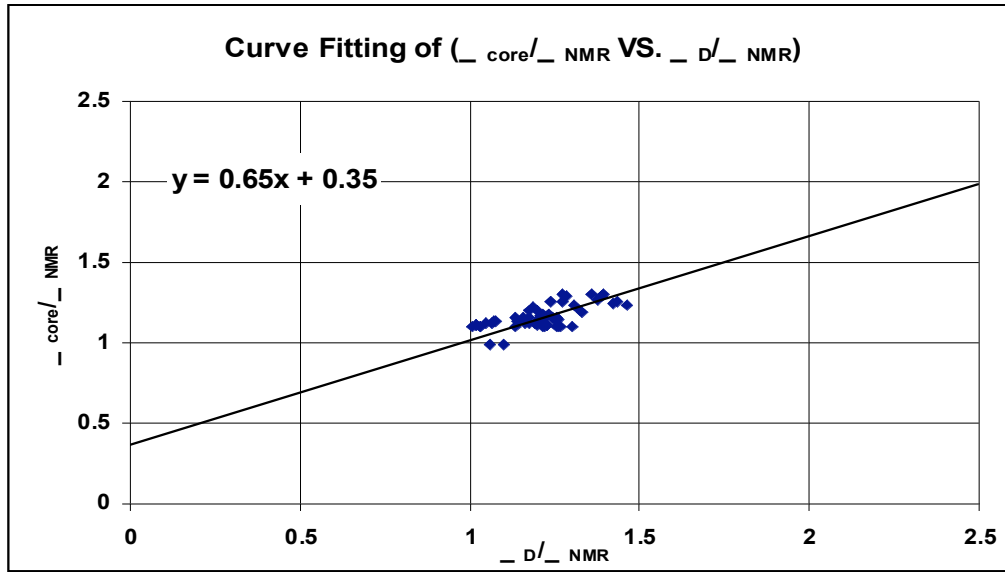


Fig. (2).  $\phi_{core}/\phi_{NMR}$  vs.  $\phi_D/\phi_{NMR}$

**Calibration for  $\phi_{DMR}$  Porosity**

A curve fitting method has been used to calibrate the A&B constants values, which are applied to the reservoir of interest. In our case, we have selected well (A) (Both core and NMR data were available over the same reservoir interval). Assuming core porosities are equal to  $\phi_{DMR}$ , which is the gas corrected porosity.

Equation 5 can be written in the following form.

$$\frac{\phi_{Core}}{\phi_{NMR}} = A * \frac{\phi_D}{\phi_{NMR}} + B \tag{6}$$

It is the linear equation intercept at B value and the slope is equal to the A value as shown in Fig. (2).

Note that at  $S_{gx0}=0$ , the pores are completely filled with liquid (mud filtrate and irreducible water), so the NMR porosity reading and density-porosity should be correct and both should equal to core porosity. As a result, the trend line should intersect at control point, where  $\phi_{Core}/\phi_{NMR} = \phi_D/\phi_{NMR} = 1$ . Fluid density for apparent  $\Phi_D$  estimation is best fitting at 0.9 g/cc, which is a combination between formation water density and mud filtrate density (OBM). The fitting trend line has a slope of  $A=0.65$  and intercepts the Y axis at  $B=0.35$ , which results in DMR porosity transform as follows:

$$\phi_{DMR} = 0.65 \phi_D + 0.35 \phi_{NMR} \tag{7}$$

**( $\phi_{DMR}$ ) Porosity Results**

The results of  $\phi_{DMR}$  transform applications in the three well A, B and C showed very good match between  $\phi_{DMR}$  and core porosities as shown in Figs. (3, 4, 5). As a result, it is considered as an independent facies porosity model. These corrected porosities can be used in conjunction with Timur-Coates equation to estimate the accurate permeability in gas bearing formations.

Figs. (3, 4, 5) present well logs, showing PHID and  $\phi_{DMR}$ . Gamma ray and Caliper curves are shown in the first track (GR&CALI), second track shows depth in meters, the third one is resistivity, the fourth one is neutron-density logs, the fifth track shows comparison between core, density and NMR porosities, sixth track shows comparison between  $\phi_{DMR}$  and core porosity, seventh track shows saturations of gas (green shadow) and water (blue shadow), and the last track shows core permeability in mD.

The DMR method has the advantage of avoiding the use of fluid density and gas hydrogen index (HI) at reservoir conditions for gas correction. Another advantage is that we can increase logging speeds as we do not need full polarization for gas.

**BULK GAS - MAGNETIC RESONANCE PERMEABILITY ( $K_{BGMR}$ )**

Permeability is derived from the empirical relationship between NMR porosity and mean values of T2 relaxation times. Two permeability models are widely used in the industry Kenyon model [ $K = c \times (\phi_{NMR})^a \times (T2)^b$ ]. Kenyon model permeability is affected by gas and OBM filtrate (non-wetting phase), and Timur-Coates model [ $K = (\phi_{NMR}/c)^a \times (BVM/BVI)^b$ ]. Timur-Coates permeability model works well in gas reservoir, but it is affected by uncertainty of BVI cut off values and wettability alteration by OBM filtrate. The next step after defining T2 cut off values is to calibrate the fitting parameters (c, a and b) for studied gas shaly sand reservoir. Permeability determination by Timur-Coates model in the case of tight heterogeneous gas shaly sand was not satisfactory due to the effect of rock facies and tightness and the significant variation of T2 values for the same facies. Estimates of Kenyon and Timur-Coates permeability both are affected by hydrocarbon and development of new model is needed to develop different permeability models [8-11].

Bulk Gas Magnetic Resonance Permeability ( $K_{BGMR}$ ) is a new technique for permeability estimation in gas reservoirs.

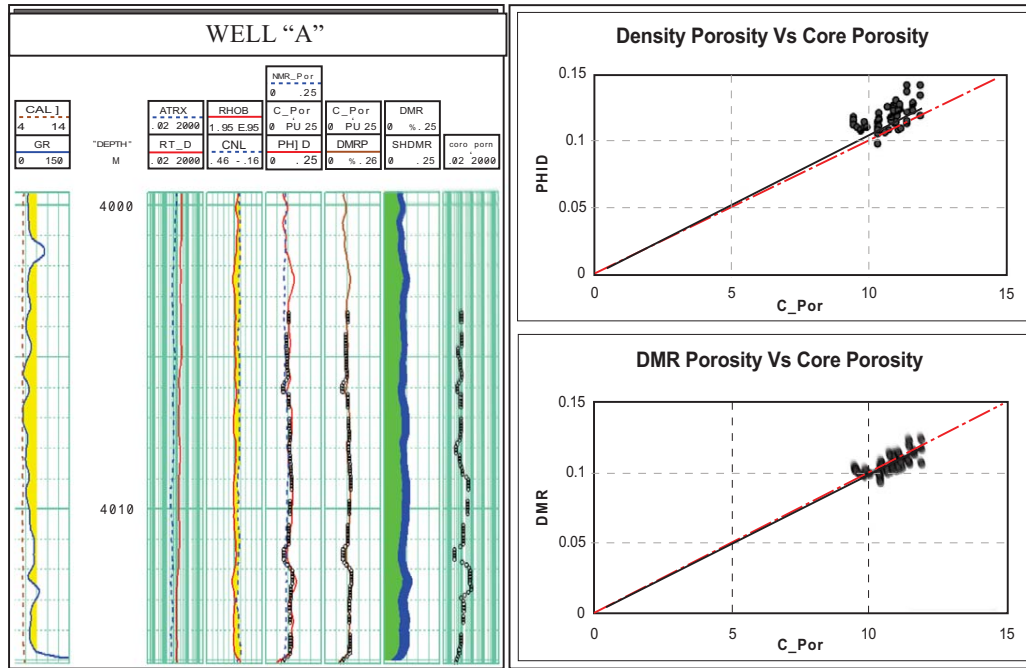


Fig. (3). On the right hand shows PHID, NMR\_Por and DMRP curves with other normal log, left hand shows PHID and DMRP correlation with core porosity in well "A".

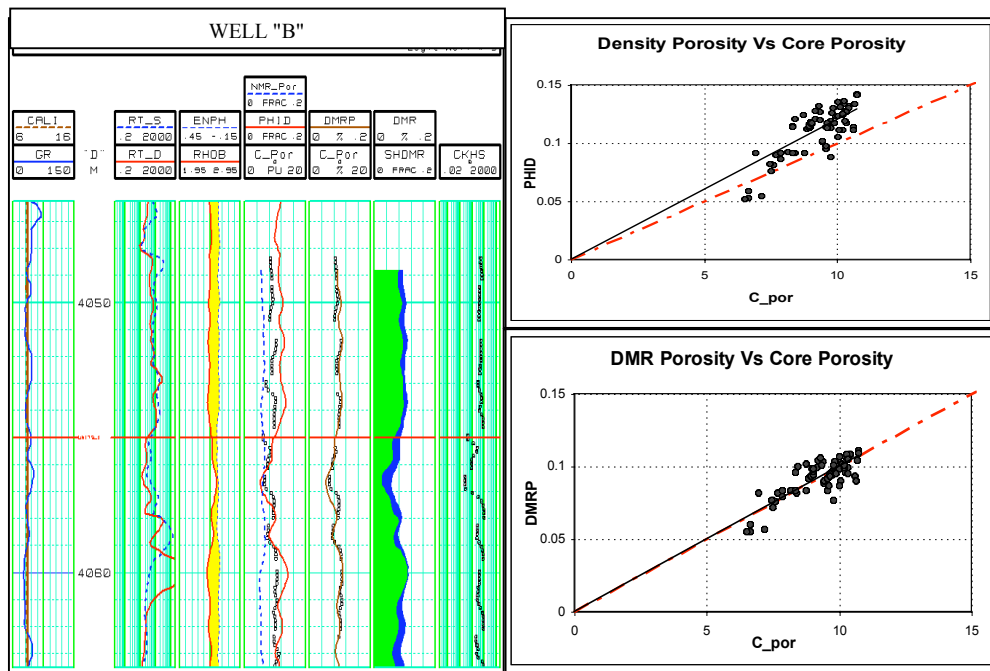


Fig. (4). On the right hand shows PHID, NMR\_Por and DMRP curves with other normal log, left hand shows PHID and DMRP correlation with core porosity in well "B".

It has the same value in OBM and WBM condition as it depends on gas re-entry to the flushed zone after mud cake take place and invasion stops.

It is a dynamic concept of gas movement behind mud cake as a result of permeability formation, gas mobility, capillarity and gravity forces. Because gravity forces are constant, capillarity depends mainly on permeability and mobility depends on permeability and fluid viscosity which is con-

stant for gas; the gas re-entry volume directly function in permeability.

**Bulk Gas Volume Calculations**

The gas volume in the flushed zone can be calculated by using different techniques as follows;

Differential spectrum ( $\Delta T_w$ )

Multi acquisition using different waiting times ( $T_w$ )

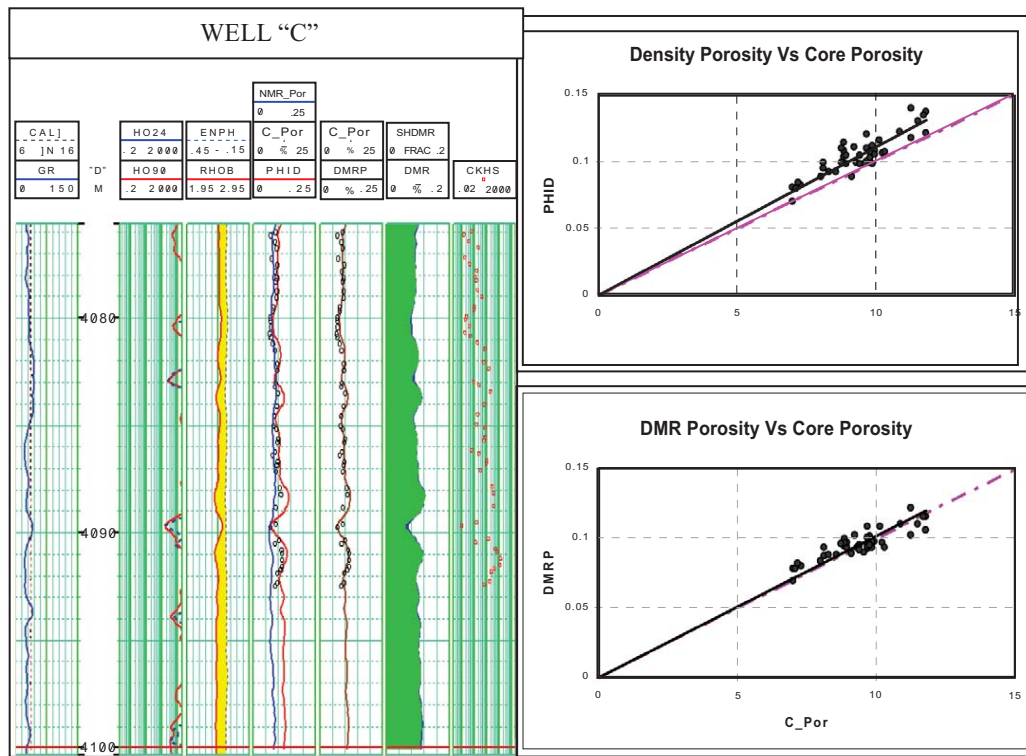


Fig. (5). On the right hand shows PHID, NMR\_Por and DMRP curves with other normal log, left hand shows PHID and DMRP correlation with core porosity in well "C".

Diffusion measurements.

2-D fluid analysis using fluid diffusivity (D) and T<sub>2</sub> spectra.

Freedman, *et al.* [6] has mathematically developed the following transform for gas volume calculation in the invaded zone.

$$V_{g,xo} = \frac{DPHI - \frac{TNMR}{(HI)_f}}{\left[ 1 - \frac{(HI)_g * P_g}{(HI)_f} \right] + \lambda}$$

V<sub>g,xo</sub> = gas volume in the flushed zone

DPHI = formation porosity from density using filtrate fluid density

T<sub>NMR</sub> = total NMR porosity

(HI)<sub>f</sub> = Fluid hydrogen index

(HI)<sub>g</sub> = Gas hydrogen index

P<sub>g</sub> = gas polarization function = 1-exp (-W/T<sub>1,g</sub>), where W is the wait time and T<sub>1,g</sub> is the longitudinal relaxation time for gas.

$$\lambda = \frac{\rho_f - \rho_g}{\rho_m - \rho_f}$$

A simple transform delivered from density tool response Eq. (2) using DMR porosity as a corrected gas porosity value is as follows.

$$S_{gxo} = \frac{(\phi_D - DMR) * (\rho_m - \rho_L)}{DMR * (\rho_L - \rho_g)}$$

Gas volume can be calculated approximately by ignoring the gas response in the NMR measurements especially in short T<sub>w</sub>, and then the approximated gas saturation in the invaded zone can be estimated as follows;

$$\text{Bulk Gas Volume (BG)} = \phi_{DMR} - \phi_{NMR}$$

### BGMR Permeability Results

Fig. (6) shows core permeability versus core porosity x-plot. It reflects how the permeability varies between facies to other within same porosity range. The last method of bulk gas volume calculation is used. The method is very simple and excluded from any complications (BG = φ<sub>DMR</sub> - φ<sub>NMR</sub>).

The same method is applied for the three wells A, B and C, and then BG is plotted versus formation permeability Fig (7). The correlation is normalized by dividing the gas volume by the total porosity of DMRP to be equal to S<sub>gxo</sub>, Fig. (8).

$$S_{gxo} = \frac{DMRP - \phi_{NMR}}{DMRP}$$

The correlation between S<sub>gxo</sub> and permeability shown in Fig. (9) has resulted in following permeability transform.

$$K_{BGMR} = 0.18 * 10^{(6.4 * S_{gxo})} \tag{8}$$

This transform is facies independent and the statistical analysis of absolute error for this correlation is about a factor of 2, this is acceptable from uncertainty assessment point of view as compared to permeability uncertainty assessment

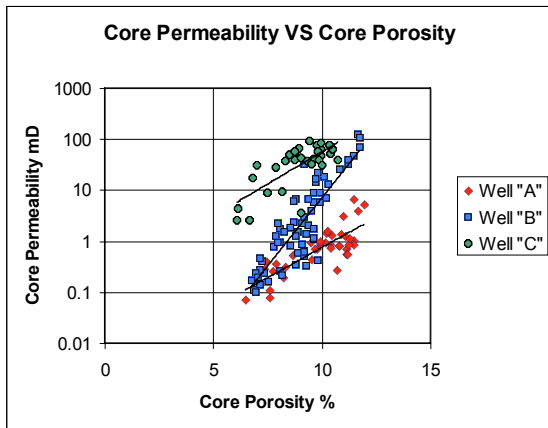


Fig. (6). Core permeability versus core porosity for three wells A,B and C.

from core por-perm transforms in the same reservoir, where the uncertainty factor ranges from 1.5-3 and depends on facies. Permeability derived using equation 7 in three wells A, B and C is shown in Figs. (9, 10, 11). All three wells A, B and C have shown a good match between  $K_{BGMR}$  permeability with core permeability.

CAPILLARY PRESSURE, ( $P_C$ )

Based on the fact that relaxation processes act in parallel, transverse relaxation time T2 takes the form:

$$1/T2 = (1/T2)_B + (1/T2)_S + (1/T2)_D \tag{9}$$

Where  $(1/T2)_B$  is the bulk contribution,  $(1/T2)_S$  is the surface contribution and  $(1/T2)_D$  is the diffusion in field gradient contribution.

In the fast diffusion limit, T2 is given by following form

$$1/T2 = (1/T2)_B + (1/T2)_S \tag{10}$$

$$1/T2 = (1/T2)_B + \rho S_{pore}/V_{pore} \approx \rho S_{pore}/V_{pore}$$

In this limit, T2 is affected by two factors: (1) the surface relaxivity  $\rho$  and features of pore body size  $r_{pore} = V_{pore}/S_{pore}$  and (2) the bulk relaxation time T2, which is much longer than the surface fluid relaxation time. Thus, the first term in Eq. (10) negligible and hence,  $T2 \approx r_{pore} / \rho$ . Because of large variations in surface properties ( $\rho$ ) among different facies and pore geometries and pattern, the standard T2 cutoff values (33ms in sandstone and 90 ms in carbonates) are not always applicable [12-15].

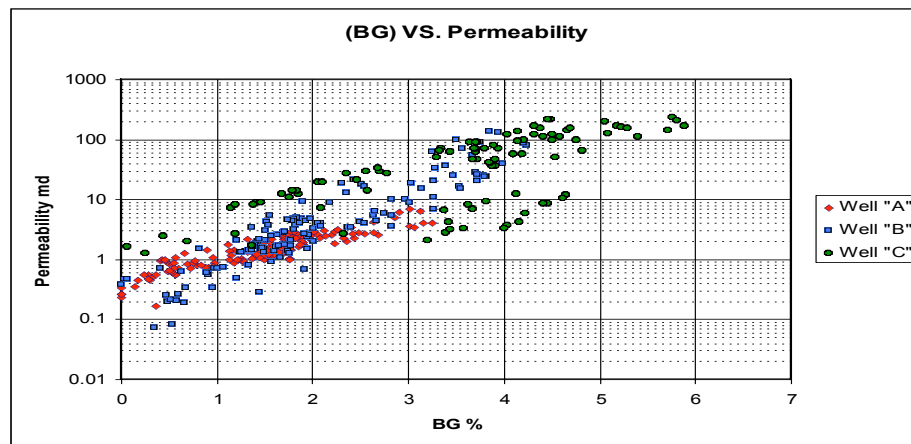


Fig. (7). BG and permeability correlation.

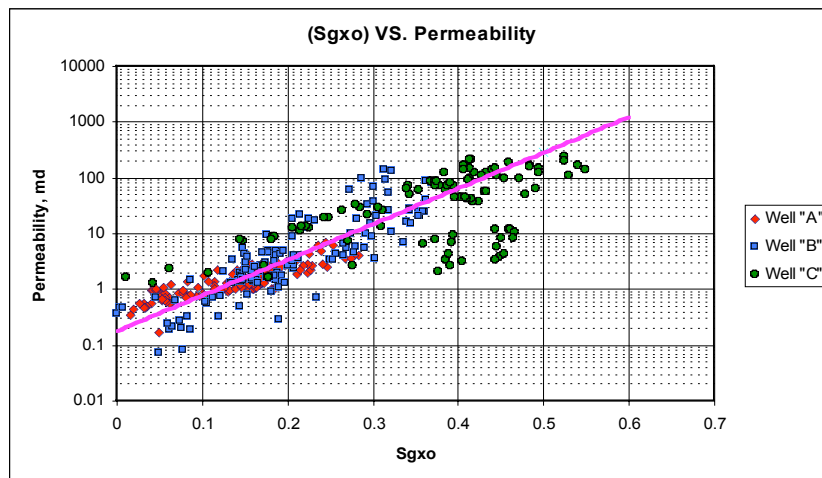


Fig. (8). Permeability versus  $S_{gxo}$  correlation.

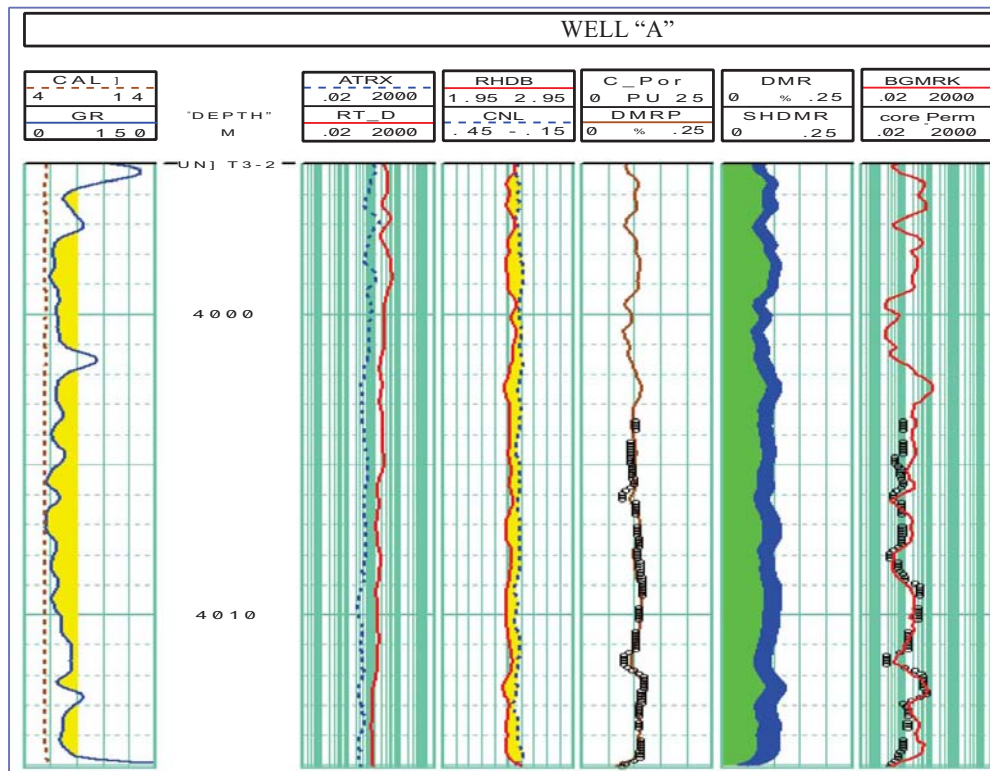


Fig. (9). BGMR permeability, track 6, red line for well A.

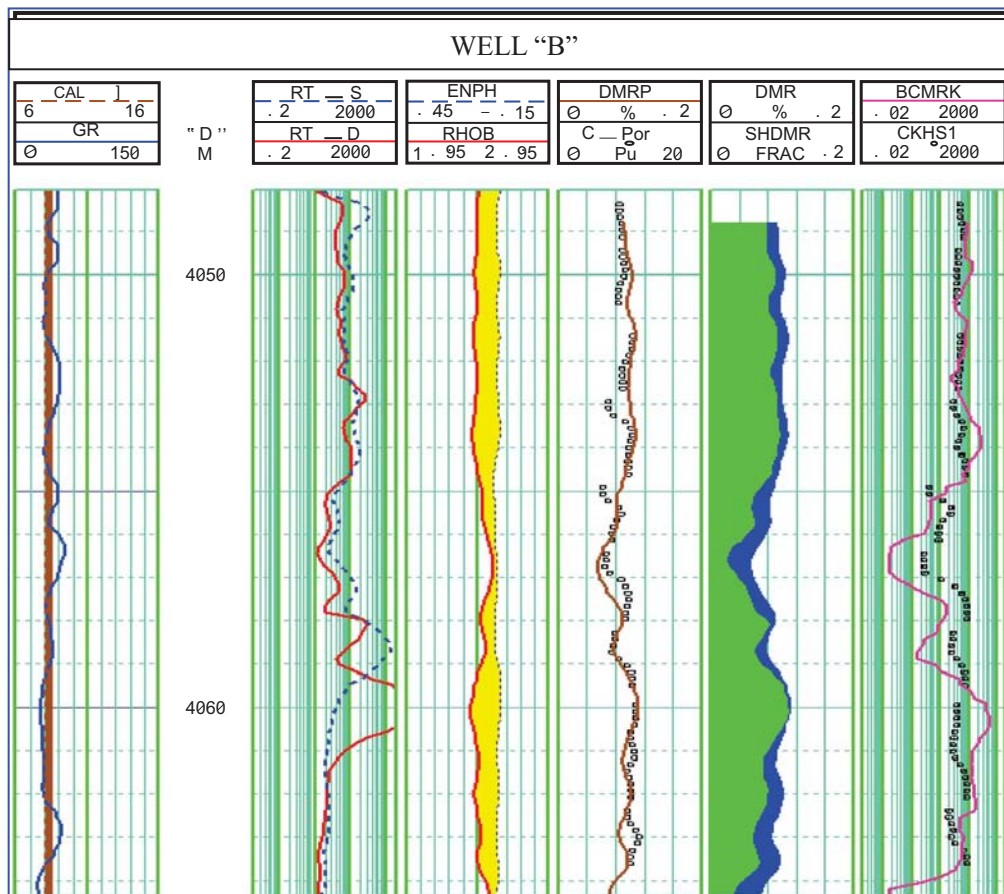


Fig. (10). BGMR permeability, track 6, purple line for well B.

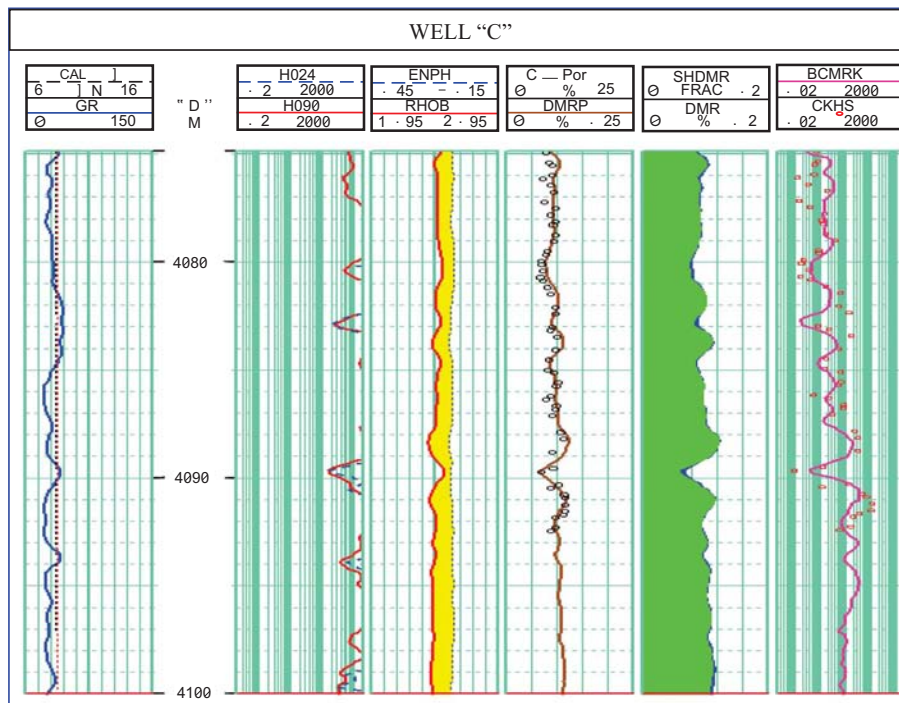


Fig. (11). BGMR permeability, track 6, purple line for well C.

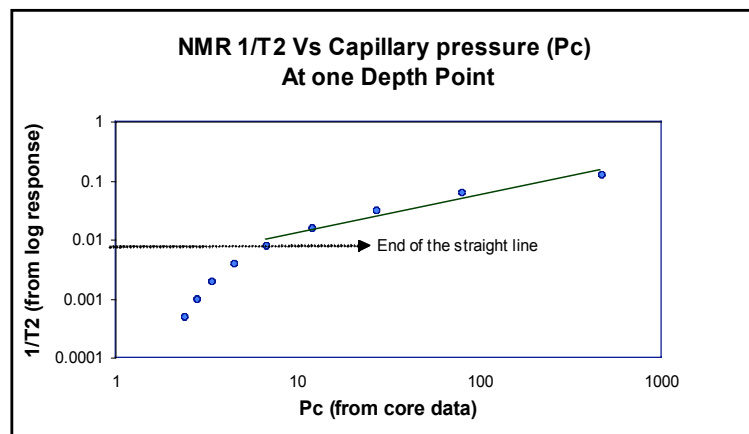


Fig. (12). 1/T2 Vs capillary pressure, Pc.

Capillary forces in a reservoir rock are related to wettability and rock surface tension works against density differences between the fluids to significantly change the previous sharp interfaces between fluids [16]. Capillary pressure (Pc) is the result of the combined effects of the interfacial tensions of fluids and rock ( $\sigma$ ), pore radius (r) and rock wettability defined by angle ( $\theta$ ), it has the following equation:

$$P_c = 2 \sigma \cos \theta / r \tag{11}$$

Since pore radius (r) is related to T2 and rock surface relaxivity ( $\rho$ ), Eq. (11) can take the following form:

$$P_c = 2 \sigma \cos \theta / T_2 \rho \tag{12}$$

For given reservoir rock ( $2 \sigma \cos \theta / \rho$ ) is constant (C), thereby Eq. (12) can take the form  $P_c = C / T_2$ .

$$\text{Log } P_c = \text{Log } C + \text{Log } 1/T_2 \tag{13}$$

The challenges in the current case are the gas bearing pores which are not presented by NMR and OBM filtrate

which partially displace  $S_{wi}$ . To avoid the risk of those two changes, the calibration of the model will be based on the formation pores which are filled with liquid and presented by NMR tools response [16-18].

**Model Calibration**

To overcome the above challenges, calibration of the model will be based on the NMR tool response of the full liquid filled pores and then correlate SCAL versus capillary pressure analysis according to the following sequence;

**T2 cut off for Gas Effect:** Regarding equation (13), the relation between log (PC) and log (1/T2) is linear under the above mentioned assumption. This is expected to get straight fitting line only in the area where NMR responses to liquid filled pores. Because of linear fitting, the extrapolation of this line is valid for both area of  $S_{wi}$  and gas bearing pores.

Fig. (12) shows straight line in the area between T2 equals 8 to 125 ms. Pores where 1/T2 is less than 0.008, is



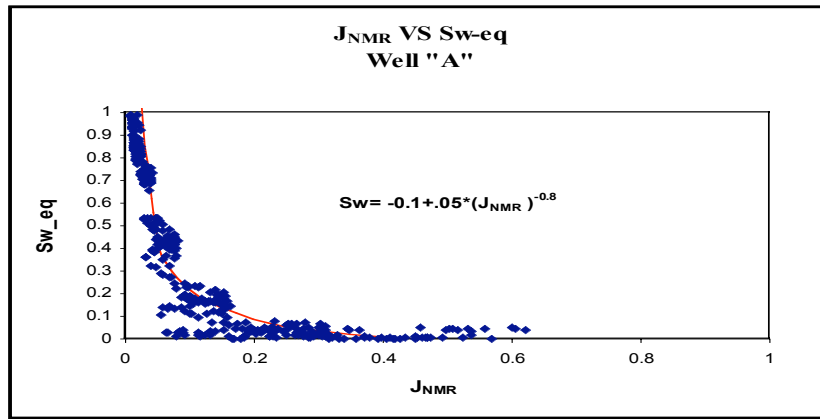


Fig. (13). Sw-eq Vs J<sub>NMR</sub> for well A.

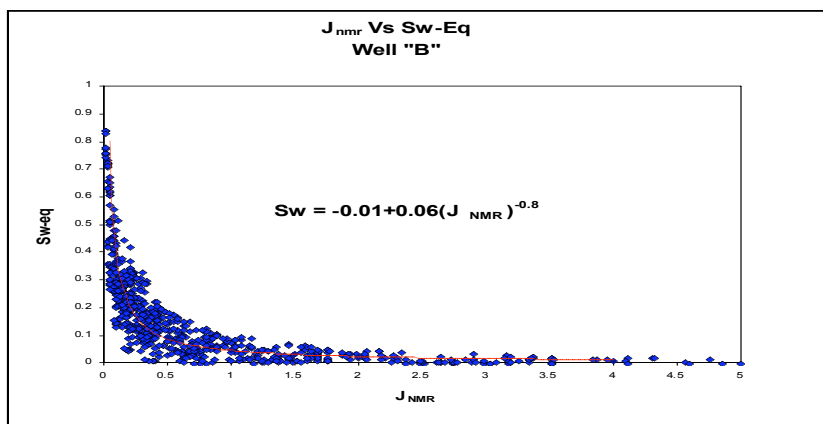


Fig. (14). Sw-eq Vs J<sub>NMR</sub> for well "B".

partially or completely filled with gas. Therefore the calibration of the model (Eq. 12) will be based on T<sub>2</sub> period from 8 to 125 ms.

**Data Averaging:** J-Leveret function is used for data averaging between T<sub>2</sub> and equivalent Sw<sub>eq</sub> from NMR, by replacing C/T<sub>2</sub> instead of P<sub>c</sub> (Eq. 13). Same averaging method is used for capillary pressure saturation-height function.

$$J_{NMR} = \frac{1}{T_2} \sqrt{\frac{perm(\kappa)}{por(\phi)}}$$

$$Sw_{eq} = Sw_i + c_1 \left[ \frac{C}{T_2 * \sigma \cos \theta} * \sqrt{\frac{perm(\kappa)}{por(\phi)}} \right]^{c_2} \quad (14)$$

Where

C<sub>1</sub>&C<sub>2</sub>: constants

σ : Interfacial tension & θ : contact angle

Obayed Saturation/ Height Function, J-Leveret function where σ cos θ is equal to 50 is;

$$Sw = 0.01 + 0.5 * \left[ \frac{Pc}{50} \sqrt{\frac{\kappa}{\phi}} \right]^{-0.8} \quad (15)$$

**Calibration Results:** Data averaging has been applied to two wells (A&B), where OBM was used while drilling reservoir section and another well (D) were drilled by water base mud (WBM)

Well "A", Fig. (13)

The resulting relationship between Sw<sub>eq</sub> and the 1/T<sub>2</sub> is as follows;

$$Sw = -0.1 + 0.05 * \left[ \frac{1}{T_2} \sqrt{\frac{\kappa}{\phi}} \right]^{-0.8} \quad (16)$$

In order to get linear correlation between P<sub>c</sub> and 1/T<sub>2</sub> from equations (15) and (16), the equivalent Sw from NMR data should be increased by 0.11 (11%). This makes sense where OBM filtrate partially replaced part from the formation water, which results in the shift increase in T<sub>2</sub> spectra. So, we can consider this forced increase in equivalent Sw by 0.11 as a correction for OBM filtrate effect.

By applying this 0.11 OBM filtrate correction, the resulting relationship between P<sub>c</sub> and T<sub>2</sub> is as follows;

$$P_c = 889 \frac{1}{T_2}$$

$$C=889$$

b) Well "B", Fig. (14)

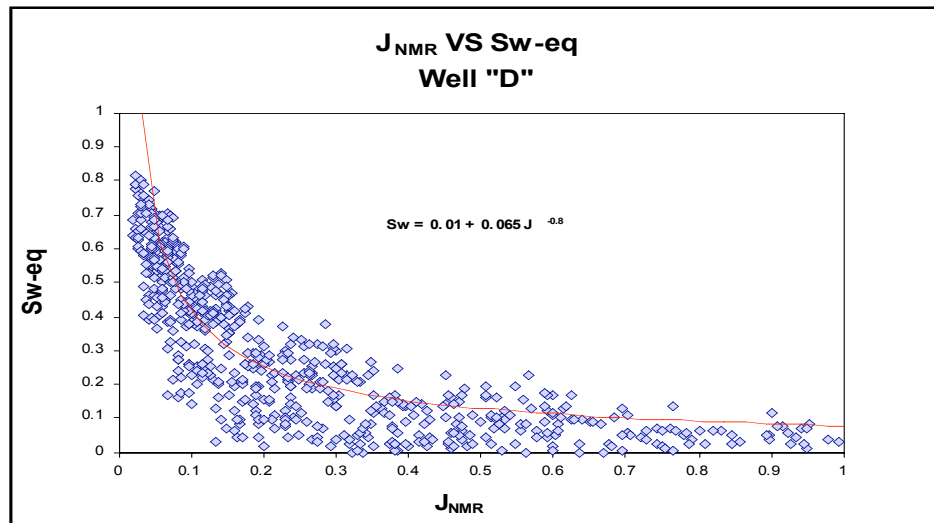


Fig. (15). Sw-eq Vs J<sub>NMR</sub> for well D.

The result and trend line equation is as follows;

$$Sw = -0.01 + 0.06 * \left[ \frac{1}{T_2} \sqrt{\frac{\kappa}{\phi}} \right]^{-0.8} \tag{17}$$

In this case, the equivalent Sw from NMR data should be increased by 0.02 in Eq. (17) as a mud filtrate correction. Then the correlation results in the following transform:

$$Pc = 708 \frac{1}{T_2}$$

$$C=708$$

Average C =800 is considered as the arithmetic mean of the above two values, in case of OBM. So, the average correlation between PC and T2 is:

$$Pc = 800 \frac{1}{T_2} \tag{18}$$

c) Well "D", Fig. (15)

The well was drilled using water base mud (WBM), which is the main difference with the previous wells "A" and "B", but there are no cores acquired.

The resulting relationship between Sw and the J<sub>NMR</sub> is as follows;

$$Sw = 0.01 + 0.065 * \left[ \frac{1}{T_2} \sqrt{\frac{\kappa}{\phi}} \right]^{-0.8} \tag{19}$$

Equation 19 shows no correction is needed for Sw. This makes sense as the well was drilled with WBM, which is adequate for NMR capillary approximation analysis.

The resulting transform between Pc and T2 is:

$$Pc = 640 \frac{1}{T_2} \tag{20}$$

### CAPILLARY PRESSURE (PC) APPROXIMATION RESULTS

#### Well "A"

Fig. (16) shows the correlation between NMR approximated capillary pressure and capillary pressure from SCAL core data. The correlation presents relatively good match for this type of low quality reservoir and OBM filtrate.

#### Well "B"

As shown in Fig. (17), the approximated capillary pressure from NMR is much closed to that of SCAL core data.

#### Well "D"

As shown in Fig. (18), the approximated capillary pressure from NMR gives good match with that of SCAL core data.

### CONCLUSIONS

#### A-DMR

##### Porosity

1-DMR porosity method is a gas corrected porosity, and independent facies porosity model. It depends on a mathematical derivation. It combines two tools responses in one simple transform.

2- DMR porosities show minimal uncertainty, because individual unknowns (RHOF and Hlg) are compensated and eliminated in the DMR transform.

#### B-BGMR Permeability

1-BGMRK is facies independent technique and this is the most important characteristic of this technique. It is simple and a new concept for permeability estimation in gas well.

2-BGMR permeability model avoids using BVI values and T<sub>2</sub> cut-off with its associated uncertainty, especially in gas reservoir and OBM conditions.

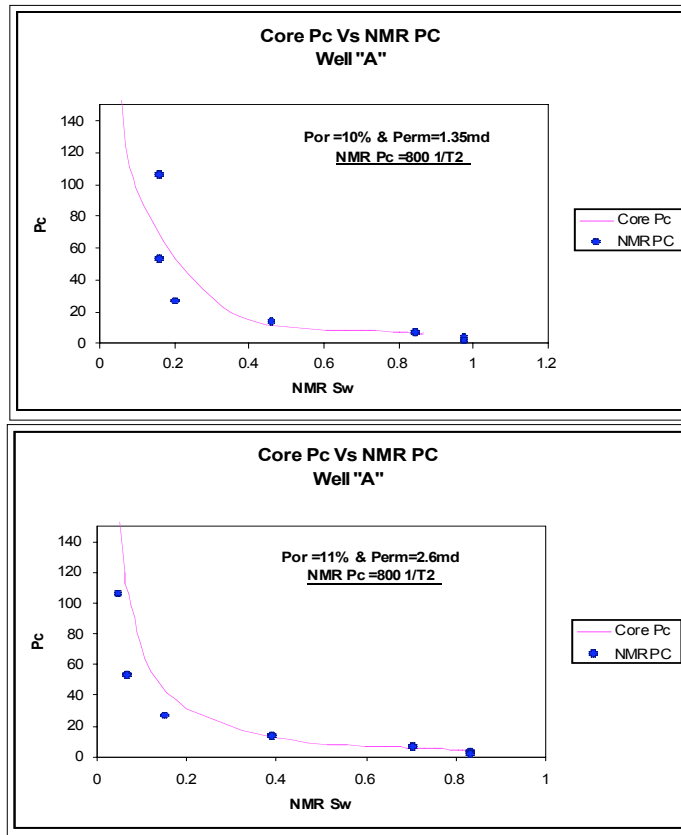


Fig. (16). NMR Pc and Core-Pc comparison in well A.

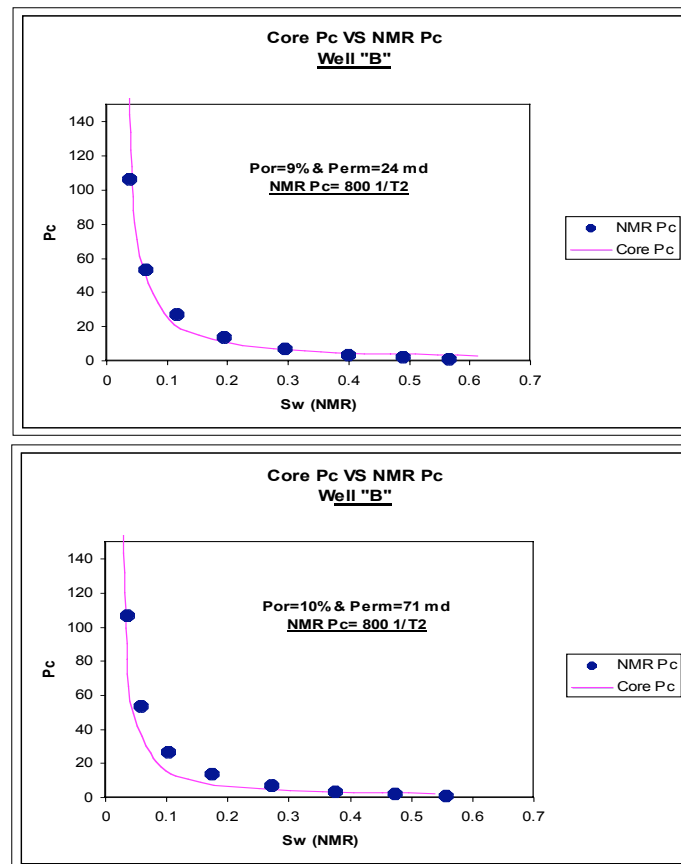


Fig. (17). NMR Pc and Core-Pc comparison in well "B".

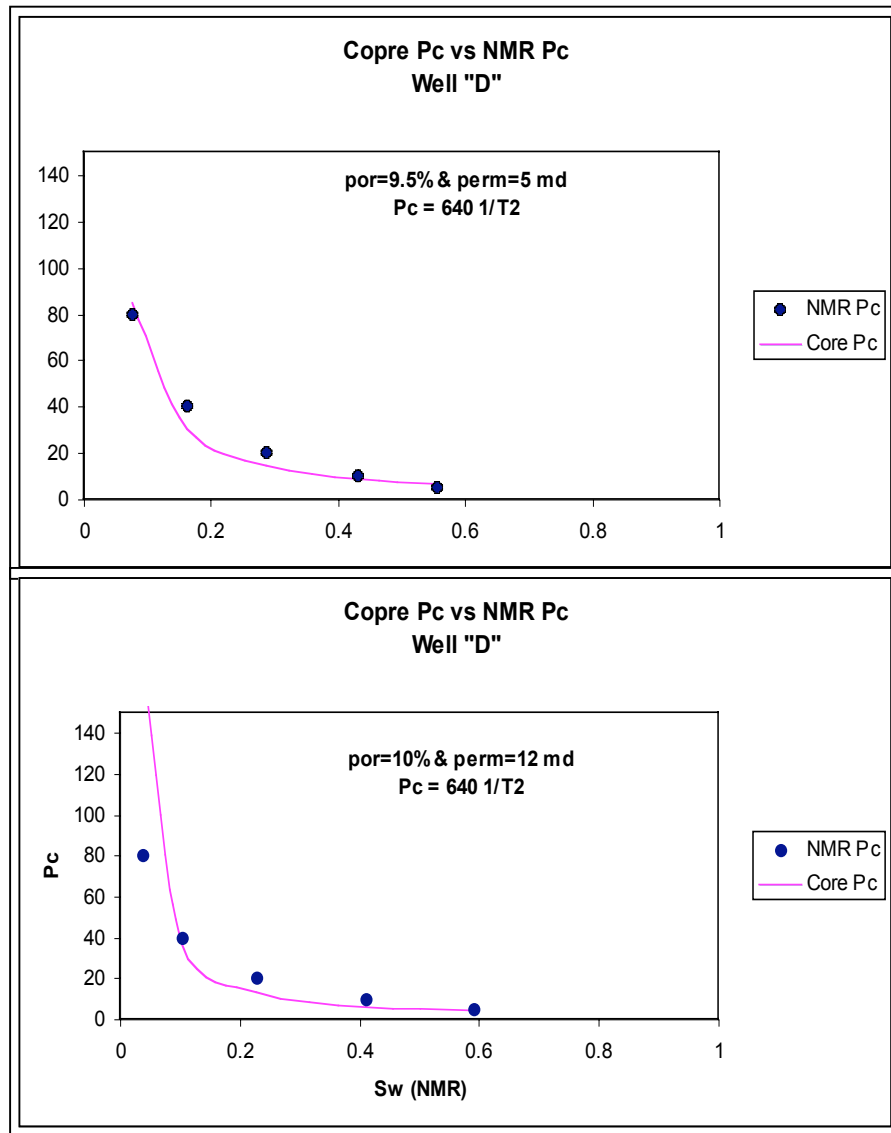


Fig. (18). NMR Pc and Core-Pc comparison in well D.

3- BGMR permeability model is valid only for gas bearing reservoir. It could not be valid in the transition zone (need further study). It is affected by fluid mobility in the invaded zone, especially in case of change in the filtrate fluid properties.

**NMR Capillary Pressure**

1-The assumptions of capillary pressure approximation from T<sub>2</sub> distribution can be applied in gas wells as well with some consideration due to gas and mud filtrate effects. Shift correction of T<sub>2</sub> spectra due to OBM filtrate can be quantified using J-Leveret function method for data averaging and regression.

2-The approximate relation between Pc and T<sub>2</sub> is  $P_c = C (1/T_2)$ . The constant C slightly depends on facies or reservoir quality and the type of drilling fluid. In case of OBM, C value ranges from 710 to 880 related to high and low quality, respectively. C=790 can be considered as an average in case of OBM. In case of WBM, C= 850 is used as the average.

3- The cap curve resulted from T<sub>2</sub> spectra can be used for saturation estimations in the transition zones. Pore size distribution and T<sub>2</sub> spectra can be corrected using core cap-curves integrated with T<sub>2</sub> spectra.

Recent and the ongoing research on the methods for inferring rock wettability from NMR looks promising. Looking further into the future, there is potential to use NMR methods to image fluids in reservoirs in the same way that magnetic resonance imaging is used in medicine to image soft tissues.

**ACKNOWLEDGMENT**

Author would like to thank King Fahd University of Petroleum & Minerals for kind support and help to accomplish this research and Bapetco for providing well logging data used in this research.

**NOMENCLATURE**

- B0 = Static magnetic field of the tool (gauss)
- B1 = Radio frequency magnetic field (gauss)

BG	= Bulk gas
$K_{BGMR}$	= Bulk gas magnetic resonance permeability
BVI	= Bulk volume irreducible
BVM	= Free-fluid volume available for hydrocarbon storage and fluid flow
CBW	= Clay bound water
SCAL	= Special core analysis
$\phi_{DMR}$	= Density-magnetic resonance porosity
DPHI	= Formation porosity from density using filtrate fluid density
$F_s$	= Pore shape factor
$HI_g$	= Gas hydrogen index
$HI_L$	= Fluid hydrogen index (water + mud filtrate)
MBVI	= Magnetic bulk volume irreducible
MBVM	= Magnetic bulk volume movable
MHPI	= Magnetic porosity
$P_c$	= Capillary pressure
$P_g$	= Gas polarization factor
$r_b$	= Radius of the pore
$r_{pt}$	= Radius of pore throat
$S_{gxo}$	= Gas saturation in the flushed zone
$S_{wi}$	= Irreducible water saturation
$S/V$	= Surface to volume ratio of the pores
T1	= Longitudinal relaxation time
$T_{1,g}$	= Gas longitudinal relaxation time
$T_2$	= Transverse relaxation time
$T_w$	= Waiting time (Fluid properties)
$V_{g,xo}$	= Gas volume in the invaded zone
W	= Wait time (actual waiting time of the NMR tool against the formation)
$\gamma$	= Gyromagnetic ratio (fluid magnetic property)
$\rho_2$	= Surface relaxation
$\sigma$	= Surface tension
$\theta$	= Fluid contact angle
$\rho_f$	= Fluid density
$\rho_b$	= Bulk density
$\rho_L$	= Liquid density (water + filtrate)

## REFERENCES

- [1] Minh, Ch.C.; Fredman, R.; Cray, S.; Cannon, D. *Integration of NMR with other openhole logs for, improved evaluation*, SPE paper 49012, SPE Annual Technical Conference and Exhibition, New Orleans, Louisiana, 27-30 September, **1998**.
- [2] Ayala, N.M.; Munoz, R.; Rice, R.; Palacios, C.; Torne, J.P.; Leuro, R.; Fam, M. *New integrated application using T1 and T2 modes of magnetic resonance in tight gas reserve A case study from Northern Mexico*, SPE paper 107634, SPE Latin America and Caribbean Petroleum Engineering Conference, Buenos Aires, Argentina, 15-18 April, **2007**.
- [3] Hamada, G.M.; Al-Blehed, M.S.; Al-Awad, M.N. *Nuclear magnetic resonance log evaluation of low resistivity sandstone reservoir by-passed by conventional logging analysis*, SPE paper 64406, SPE Asia-Pacific oil & gas conference, Brisbane, Australia, 16-19 October, **2000**.
- [4] Coates, G.R.; Menger, S.; Prammer, M.; Miller, D. *Applying total and effective NMR porosity to formation evaluation*, SPE paper 38736, SPE Annual Technical Conference, San Antonio, 11-14 October, **1997**.
- [5] Riviere, Ch.; Roussel, J.C. Principle and potential of nuclear magnetic resonance applied to the study of fluids in porous media. *Revue IFP*, **1992**, 47, 503-523.
- [6] Freedman, R.; Minh, C.C.; Gubelin, G.; Freeman, J.J.; McGinness, T.; Terry, B.; Rawlence, D. *Combining NMR and density Logs for Petrophysical Analysis in Gas-Bearing Formations*, paper II, SPAWLA 39<sup>th</sup> Annual Meeting, Colorado, 26-29 May, **1998**.
- [7] Abushanab, M.A.; Hamada, G.M.; Oraby, M.E.; Abdelwaly, A.A. *DMR technique improves tight gas sand porosity*, *Oil Gas Jr.* **2005**, pp.12-16.
- [8] Galarza, T.; Giordano, S.; Fontanarosa, M.; Saubidet, M.; Altunbay, M.; Saeverda B.; Romero P. *Pore-scale characterization and porosity analysis by integration of NMR and openhole logs-A verification study*, SPE paper 108068, Latin American and Caribbean Petroleum Engineering Conference, Buenos Aires, Argentina, 15-18 April, **2007**.
- [9] Kenyon, B.; Kleinberg, R.; Straley, C.; Gublin, G.; Morris, C. *Nuclear magnetic resonance imaging-technology for 21<sup>st</sup> century*, Autumn, **1995**, pp.19-32.
- [10] Sen, P.N.; Straley, C.; Kenyon, W.E.; Whittingham, M.S. Surface-to-volume ratio, charge density, nuclear magnetic relaxation and permeability in clay-bearing sandstones. *Geophysics* **1990**, 55(1), 61-69.
- [11] Singer, G.M. *Fast NMR logging for bound fluid and permeability*, Paper YY, SPWLA 39<sup>th</sup> Annual Meeting, Colorado, 26-29 May, **1998**.
- [12] Sarwaruddin, M.; Skauge, A.; Torsaeter, O. *Modelling of capillary pressure for heterogeneous reservoirs by a method J-function*, SCA paper 2001-35, SCA International Symposium, Edinburgh, 16-19 May, **2001**.
- [13] Agut, R.; Levallois, B.; Klopff, W. *Integrating core measurements and NMR logs in complex lithology*, SPE paper 63211, SPE Annual Technical Conference and Exhibition, Dallas, Texas, 1-4 October, **2000**.
- [14] Songhua, C.; Ostrof, G.; Geotgi, D.T. *Improving estimation of NMR log T2 cutoff value with core NMR and capillary pressure measurements*, SCA paper 9882, SCA International Symposium, The Hague, The Netherlands, 5-8 May, **1998**.
- [15] Hassoun, T.H.; Zainalabedine, K.; Minh, C.C. *Hydrocarbon detection in low contrast resistivity pay zones, capillary pressure and ROS determination with NMR logging in Saudi Arabia*, SPE paper 37770, Middle East Oil Show, Bahrain, 15-18 March, **1997**.
- [16] Baldwin, B.A.; Yamanashi, W.S. *Capillary-pressure determination from NMR images of centrifuged core plugs: Berea sandstone*, *The Log Analyst* Sept-Oct., **1991**, pp. 550-556.
- [17] Freedman, R. *Advances in NMR logging*, JPT-January, **2006**, pp. 60-66
- [18] Hou, B.L.; Coates, G.R. *Nuclear magnetic resonance logging methods for fluid typing*, SPE paper 48896, SPE International Conference and exhibition, Beijing, China, 2-5 November, **1998**.

Received: September 16, 2008

Revised: November 10, 2008

Accepted: November 19, 2008

© G.M. Hamada; Licensee Bentham Open.

This is an open access article licensed under the terms of the Creative Commons Attribution Non-Commercial License (<http://creativecommons.org/licenses/by-nc/3.0/>) which permits unrestricted, non-commercial use, distribution and reproduction in any medium, provided the work is properly cited.